RSC Advances

PAPER

View Article Online
View Journal | View Issue

Cite this: *RSC Adv.*, 2026, **16**, 19885

Photophysical studies of diazines: effects of solvents and complexation with Cu^{2+}, Ni^{2+}, Co^{2+} and Pb^{2+} ions

Packirisamy Kuzhalmozhi Madarasi and Chinnappan Sivasankar *

The detection of toxic metal ions, such as Pb^{2+}, has become important because they cause several health issues. This study describes the photophysical properties displayed by a few symmetrical diazine compounds and the influence of solvent polarity on their emission spectra. It is noted that λ_{em} increases with an increase in the polarity of the solvent. The study of the complexation of diazine compounds with metal ions, such as Cu^{2+}, Ni^{2+}, Co^{2+} and Pb^{2+}, shows that the coordination of the metal ions to the diazine molecule induces a blue shift in the UV-visible absorption spectrum. Among the studied compounds, compound 1 exhibited the maximum emission (λ_{em}) in hexane at 309 nm, with a maximum quantum yield (Φ_{em}) of 0.0576. The metal interaction study shows that the absorption intensity of compound **1** reached the maximum for Pb, indicating that the synthesized diazine could serve as a potential molecule to detect Pb^{2+} ions. The experimental results were further supported by computational studies, and the experimental data were in good agreement with the theoretical data. The TDDFT study shows that for all the compounds, the λ_{abs} corresponds to the HOMO−1 to LUMO+1 transition.

Received 24th January 2026
Accepted 27th March 2026

DOI: 10.1039/d6ra00637j

rsc.li/rsc-advances

Introduction

The chemistry of the photophysical properties exhibited by diazines is very interesting. In the past two decades, the study of the photophysical properties of diazines has gained interest due to their widespread application in OLEDs.[1,2] Diazine compounds have also found applications in liquid crystal- and twisted-nematic-displays,[3] ion-selective optical sensors,[4] conducting materials,[5] dye lasers, image recording materials,[6] supramolecular chemistry,[7] applications of materials[8] and hole-transport materials in optoelectronic devices.[9] Diazines can also be used to bind small molecules: the lone pair on the nitrogen atom of the diazine molecule can be protonated,[10] which in turn can facilitate binding to small molecules *via* hydrogen bonding.[11] Diazines can also be used as colorimetric sensors for transition metal cations, owing to their complexation abilities with metal cations,[1,12,13] especially, to a greater extent, with 3d and 4f metal ions;[14] they also have the capability of directing metalation.[15] Diazine-mediated transition metal complexes are of much importance due to their good emissive property,[16] and diazines are efficient in binding to metal sites in well-defined arrays and placing the metal ions in close proximity, which can facilitate effective magnetic communication.[17] Thus, the interesting magnetic properties of diazines are controlled by the rotation angle of their N–N bond.[18] In particular, the magnetic properties displayed by binuclear copper(II) diazine complexes have received much attention. The magnetic interactions of Cu(II) diazine complexes are sensitive to the torsion angle about the N–N single bond of diazines, the bond angle at the two nitrogen atoms, and the nature of the functional groups attached to the diazine moiety.[19] Diazine systems are known to show significant solvatochromic behavior due to the solute–solvent interaction.[20] In particular, π-conjugated diazines exhibit good fluorescence properties and emission solvatochromism.[21] The intermolecular charge transfer (ICT) scaffolds in the diazine compounds induce the photoluminescence property in them, which depends on the polarity of the solvent,[21–29] the pH of the solution[23–29] and the chelated metal ions.[30,31] The electronic absorption spectra of diazines are also greatly influenced by the polarity of the solvent.[32] The blue shift of the n–π* transition with respect to solvent polarity is a topic of great interest in diazine systems.[33] In addition, diazine units are incorporated as π-linkers in push–pull chromophores for photovoltaic applications; due to the significant π-deficient character of diazine heterocycles, they can be used as electron-withdrawing groups in push–pull structures.[33,34] Considering the broad potential applications of diazines across various fields, this study examines the effect of solvent polarity on the absorption and emission behaviour of a few diazine molecules and the influence of metal ions on their absorption and emission spectra.

Catalysis and Energy Laboratory, Department of Chemistry, Pondicherry University (A Central University), Puducherry 605014, India. E-mail: siva.che@pondiuni.ac.in

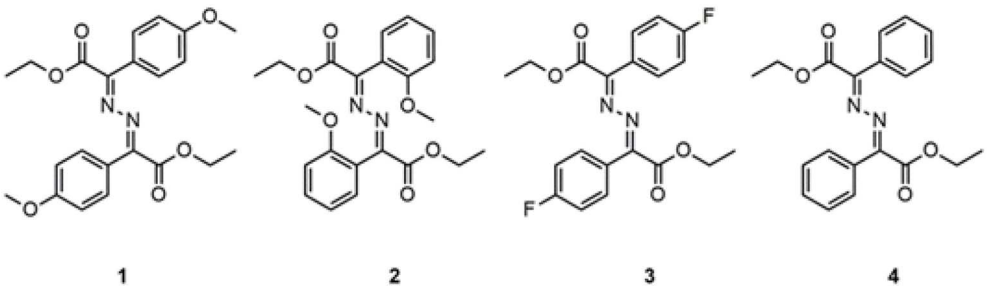

Scheme 1 Structures of the diazine derivatives used for photophysical studies.

Results and discussion

The diazine derivatives, (2*E*,2′*E*)-diethyl-2,2′-(hydrazine-1,2-diylidene)bis(2-(4-methoxyphenyl)acetate) (**1**), (2*E*,2′*E*)-diethyl-2,2′-(hydrazine-1,2-diylidene)bis(2-(2-methoxyphenyl)acetate) (**2**), (2*E*,2′*E*)-diethyl-2,2′-(hydrazine-1,2-diylidene)bis(2-(4-fluorophenyl)acetate) (**3**) and (2*E*,2′*E*)-diethyl-2,2′-(hydrazine-1,2-diylidene)bis(2-phenylacetate) (**4**), were synthesized using the reported procedure (Scheme 1).[35] Among the synthesized compounds, diazine derivatives **1–3** displayed fluorescence behaviour in hexane (Fig. 1). Hence, the photophysical properties of these derivatives were studied and compared with those of the unsubstituted diazine derivative, (2*E*,2′*E*)-diethyl-2,2′-(hydrazine-1,2-diylidene)bis(2-phenylacetate) (**4**); herein, the results are reported.

UV-visible and fluorescence spectroscopy

The UV-visible and photoluminescence (PL) spectroscopic data for the synthesized diazine derivatives **1–4** were studied using different solvents with varying polarities at 25 °C at a concentration level of 1 μM, and the results are summarized in Table 1.

The absorption maxima (λ_{max}) in the UV-visible spectra are in the range of 280–320 nm. The absorption spectra show that the polarity of the solvent does not have much influence on the absorption maxima of the synthesized compounds (Fig. 2 and Table 1). In the case of **1** and **2**, in addition to the absorption maxima, second and third absorptions at higher energies were also observed, attributed to π–π*.

However, the λ_{max} in the emission spectra of the synthesized compounds increases with an increase in the polarity of the solvent, which is in accordance with the Dimroth–Reichardt polarity

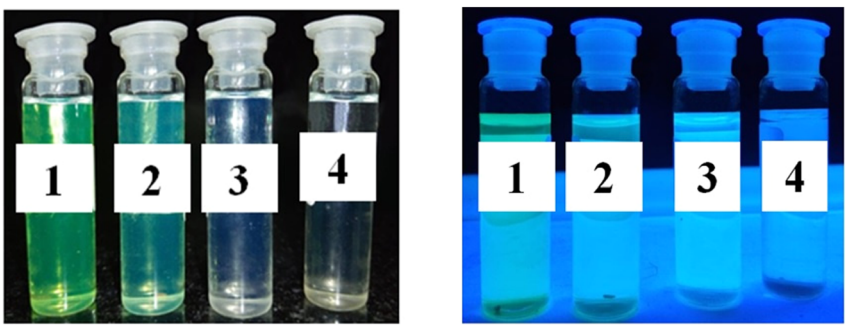

Fig. 1 Fluorescence behaviour of compounds **1–4** in hexane.

Table 1 Solvent effect on the photophysical properties of the synthesized compounds; λ_{max} (nm) corresponding to the UV-vis and emission spectra of the compounds **1–4**

	1		**2**		**3**		**4**	
Solvent system	UV-vis	PL	UV-vis	PL	UV-vis	PL	UV-vis	PL
CH_3OH	277, 227	434, 412	318, 253	399	284	399, 363	312	405
CH_3CN	298, 277, 230	382, 304	321, 255	378	319	383, 353	312	372
DMSO	300, 233	372, 312	324, 256	374	320	381, 353	318	370
DCM	280, 229	362, 283	319, 258	365	318	370, 310	315	362
THF	282, 233	358, 318	317, 260	357	304	362	312	346
Hexane	288, 229	309	318, 249	349	309	348	310	329

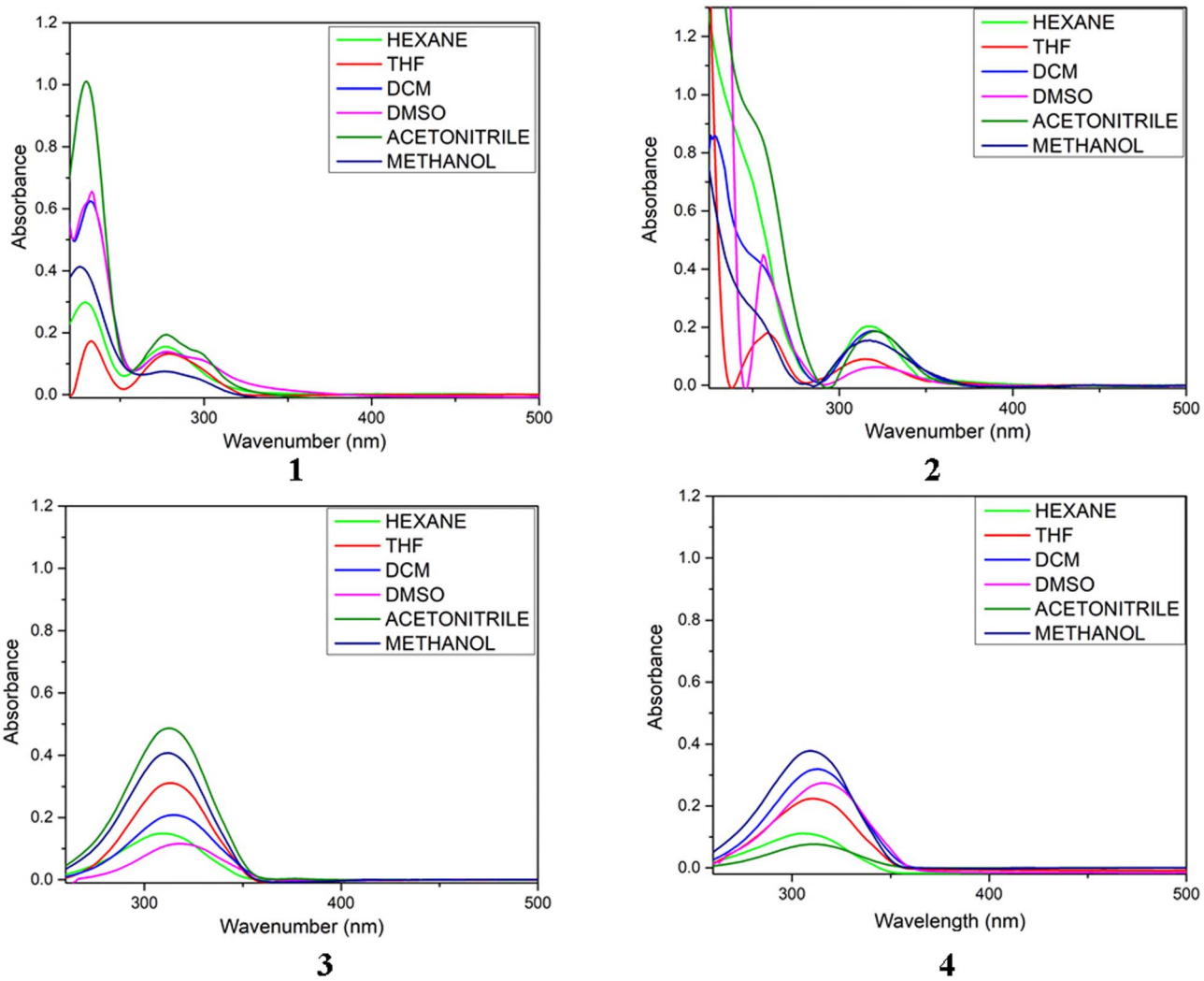

Fig. 2 UV-visible spectra of the compounds 1–4 in various solvents.

parameter ($E_T(30)$) (Fig. 3 and Table 1).[36] The effect of solvent polarity on the fluorescence properties of the compounds was studied using the slope (SP) of the regression line of the λ_{em} plot *versus* the Dimroth–Reichardt polarity parameter ($E_T(30)$) (Fig. 4).

The plot shows good linearity for all the compounds. Simultaneously, a decrease in the fluorescence intensity was also observed with an increase in the polarity of the solvent (Fig. 4). The experimental values are in good agreement with the theoretical values. A broad, structureless emission spectrum is observed for the compounds in polar solvents, attributable to the internal charge transfer (ICT) on excitation, which leads to the stabilization of the emitting state by polar solvents.[37] However, the comparatively non-polar solvent, hexane, showed a well-defined emission spectrum, which might be attributed to the partial aggregation of chromophores.[38]

Stokes shift

Stokes shift is a solvent-polarity-dependent factor. A large Stokes shift was observed for high-polarity solvents, and the Stokes shift decreases with a decrease in the solvent polarity (Table 2).

Fluorescence quantum yield

The quantum yield was calculated for **1**, which showed a good fluorescence property. The emission quantum yield (Φ_{em}) calculated with reference to 2-amino pyridine ($\lambda_{abs} = 285$ and $\Phi_{em} = 0.60$) in different solvents was in the range of 57.6×10^{-3}–1.4×10^{-3}. Among them, hexane showed the maximum emission and quantum yield (Φ_{em}) (Table 3).

Influence of metal ions on the photophysical properties of diazine derivatives

Signalling the presence of metal ions and the formation of polynuclear coordination complexes are important properties of diazines, especially those of the open type. Hence, the photophysical properties of the diazine derivatives in the presence of different metal ions, such as Cu, Co, Pb and Ni, were studied. The influence of the metal ions on the absorption spectra of the

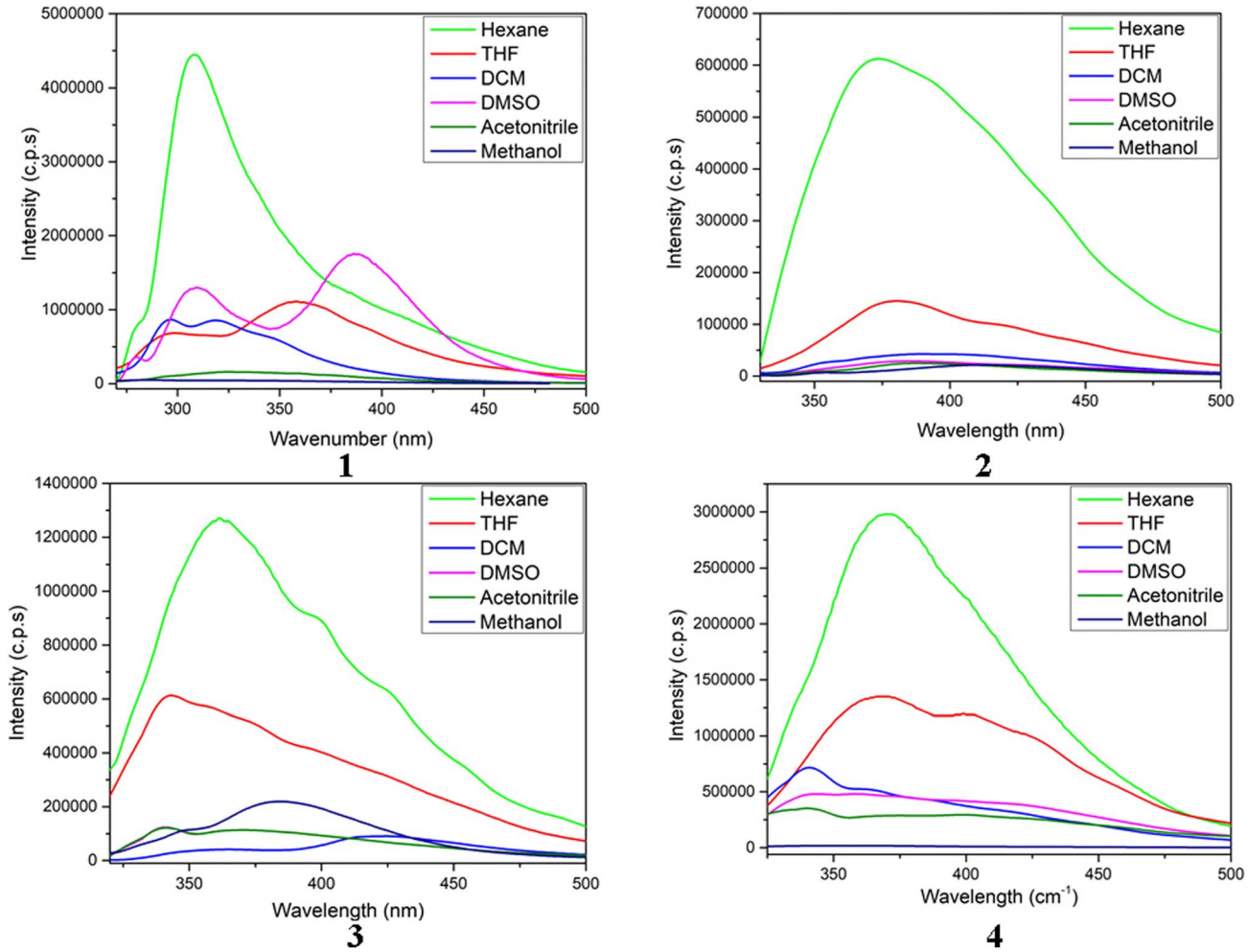

Fig. 3 Emission spectra of the compounds 1–4 in various solvents.

diazine derivatives was determined by adding a 1 mM DCM solution of metal ions into the diazine solution; DCM was chosen as the solvent because all the metal salts are completely soluble in it (Fig. 5). The addition of the metal ions produced a blue shift in the absorption spectra. The absorption intensity of the solution after the addition of the metal ions increased with a simultaneous shift towards relatively low energies (Fig. 5). Among all the metal ions used, Pb showed the maximum absorption intensity, which implies that the synthesized diazine is efficient in tracing Pb, which will be helpful for detecting heavy-metal poisoning (Fig. 5). The maximum absorption shown by Pb might be attributed to the stable complex formation ability of Pb with N-containing ligands due to its relatively soft Lewis acidic character. However, Cu showed a different absorption pattern; a well-defined MLCT band was observed at $\lambda_{max} = 218$ nm (Fig. 5). The Cu(II) ion, being a d^9 system, is known to undergo the Jahn–Teller distortion, which in turn can lead to B2 → E1, B2 → B2 and B2 → A1 transitions. Hence, it could produce a UV-vis absorption spectrum with three absorption peaks, showing that the copper ion underwent complexation with the ligand. The influence of metal ions on the absorption spectra of diazine was calculated for different concentrations of metal ions; it was observed that diazine could detect metal ions up to a low concentration of 0.001 mM (Fig. S1). The emission spectra show that the emission intensity decreased upon the addition of metal ions (Fig. 6).

Although metal-ion sensing studies use a comparatively higher concentration of metal ions (0.001 mM), a single diazine unit (monomer) exhibits good sensitivity toward metal ions. However, the reports claim that either a polymeric diazine system or a substituted diazine system could enhance the metal-ion sensing property.[39] Hence, tuning the diazine unit either by increasing the monomeric unit or adding substituents could increase the metal sensing property using a minimal concentration.

Density functional theory (DFT) calculations

TDDFT calculations were carried out with the Gaussian 09 program, using the B3LYP method[40–42] and the 6-31G* basis set.[43–47] The influence of solvent polarity on the absorption and emission behaviour was investigated using the self-consistent reaction field (SCRF) approach, specifically employing the

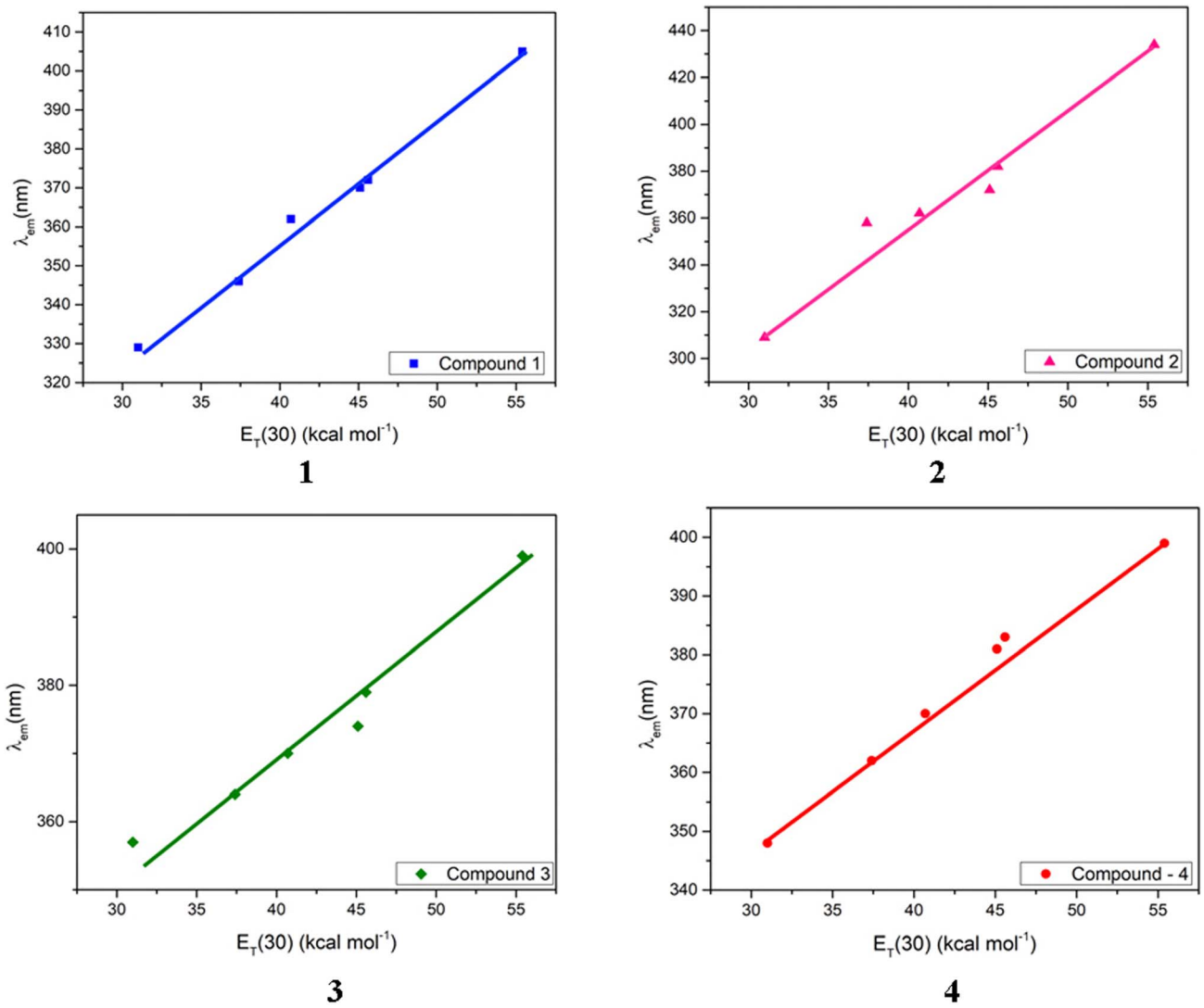

Fig. 4 Emission maxima (λ_{em}) as a function of the Dimroth–Reichardt polarity parameter ($E_T(30)$) for the compounds **1–4**.

Table 2 Stokes shift for the compounds **1–4** in different solvents

Solvent system	1	2	3	4
CH_3OH	13 060	6380	10 150	7360
CH_3CN	7380	4700	5240	5170
DMSO	6450	4130	5010	4420
DCM	8090	3960	4410	4120
THF	7530	3530	5270	3150
Hexane	2360	2790	3630	1850

Table 3 Absorption, emission and quantum yield of the compound '**1**' in different solvents

Solvent system	Absorption λ_{max} (nm)	Emission λ_{max} (nm)	Quantum yield (Φ_{em})
CH_3OH	287	434	0.0014
CH_3CN	297	382	0.0032
DMSO	311	372	0.0089
DCM	291	362	0.0053
THF	296	358	0.0070
Hexane	277	309	0.0576

polarizable continuum model (PCM).[48–52] Within the PCM framework, the solvent polarization induced by the solute's electronic charge distribution is described by means of apparent charges placed on the surface of the cavity. A high dielectric constant reflects a strongly polarizable medium, which generates an intense reaction field that effectively stabilizes charged or polar solute species. Natural population analysis (NPA) and bond order calculations have been performed using the same level of theory and basis sets. MO calculation was performed on the optimized structure to locate the FMOs of the complexes. All these computational procedures have been conducted as implemented in the Gaussian-09 package. The FMOs and geometries have been taken from the GaussView 5.0 package.[53] In order to check the reliability of

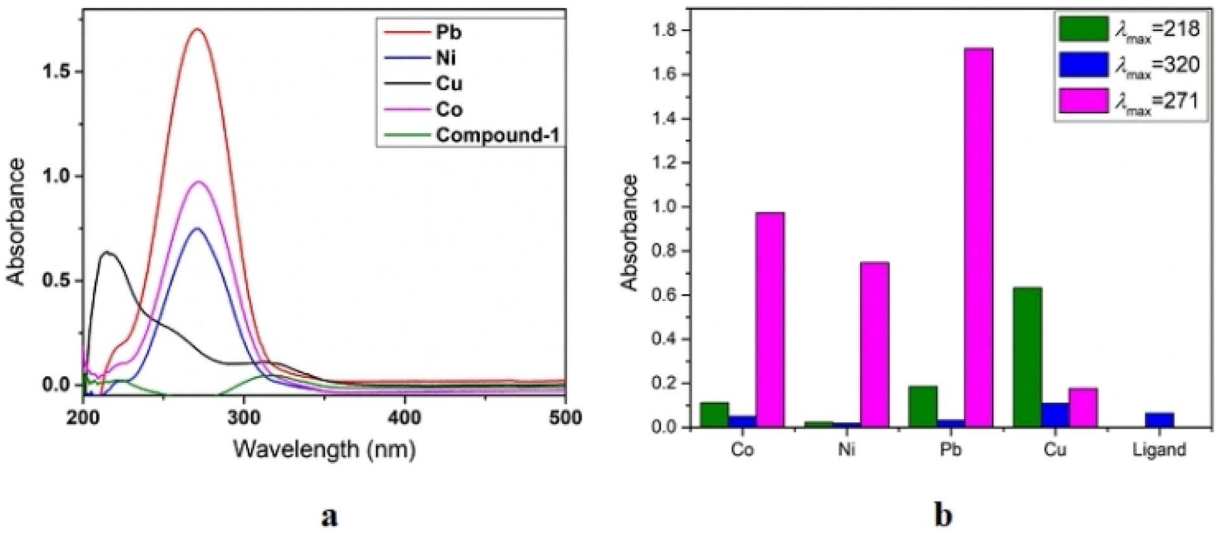

Fig. 5 (a) Absorption spectra of **1** after the addition of metal ions. (b) Bar diagram displaying the change in its absorption intensity after the addition of metal ions.

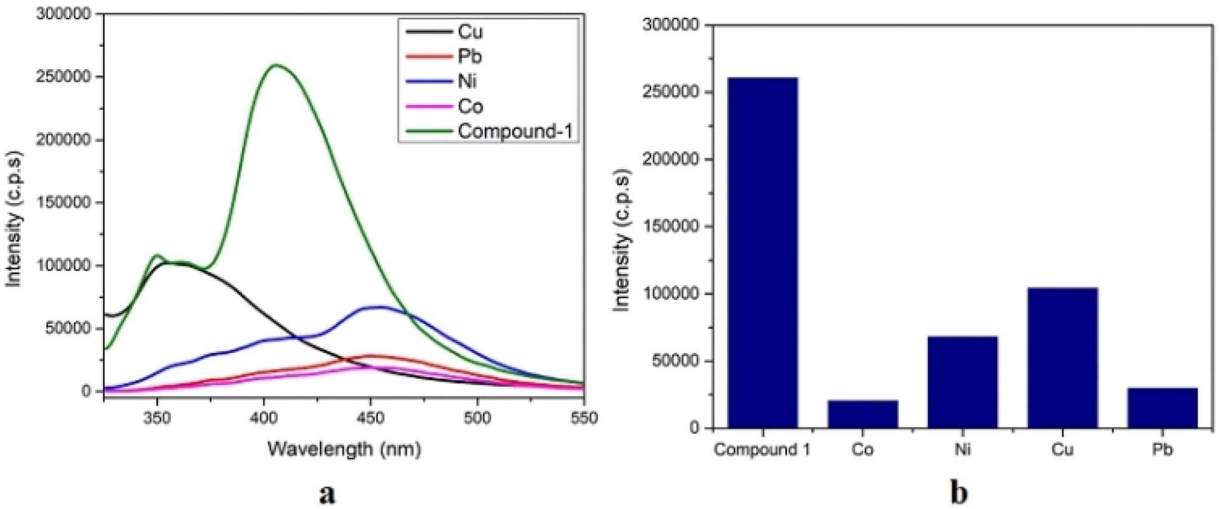

Fig. 6 (a) Emission spectra of **1** after the addition of metal ions. (b) Bar diagram displaying the influence of metal ions on the emission intensity of the compound **1**.

B3LYP/6-31G* for excited states, compounds **1–4** were optimized (Fig. S2, S3 and Table S2), TDDFT calculations were performed using CAM-B3LYP in hexane, and the observed absorption values were correlated with the results obtained from TDDFT/B3LYP.[54] Fig. 7 represents the optimized geometries of compounds **1–4**. The DFT calculation shows that for compounds **1–4**, λ_{max} corresponds to the HOMO−1 to LUMO+1 transition (Fig. S6). For compounds **1** and **2**, the difference between the experimental and calculated λ_{max} values is in the range of 2–23 nm (Table 4). In particular, DFT studies show that for **1** and **2** in all solvents, in addition to the absorption maxima corresponding to the experimental values, there is another absorption band at a lower energy, which describes the transition from HOMO to LUMO with a greater oscillator strength. This effect likely arises from the extended conjugation/delocalization of electrons imparted by the $-OCH_3$ substituents in compounds **1** and **2**, which indicates the maximum probability of the molecule to undergo a transition, with an increased photon–matter interaction. These results in turn support that **1** and **2** could be potential photosensitive materials, dyes or sensors. For **3**, the λ_{max} difference between the experimental and computed values is in the range of 5–20 nm, corresponding to the transition from HOMO−1 to LUMO+1 (Table 4). In the case of **4**, the difference between the experimental and calculated λ_{max} values is in the range of 1–6 nm. The simulated UV-vis spectrum of **1–4** using the B3LYP (in different solvents) and CAM-B3LYP (in hexane) theories is given in SI (Fig. S4 and S5). The FMO analysis shows that λ_{max} corresponds to the transition from HOMO−1 to LUMO+1 for all solvents (Table 7).

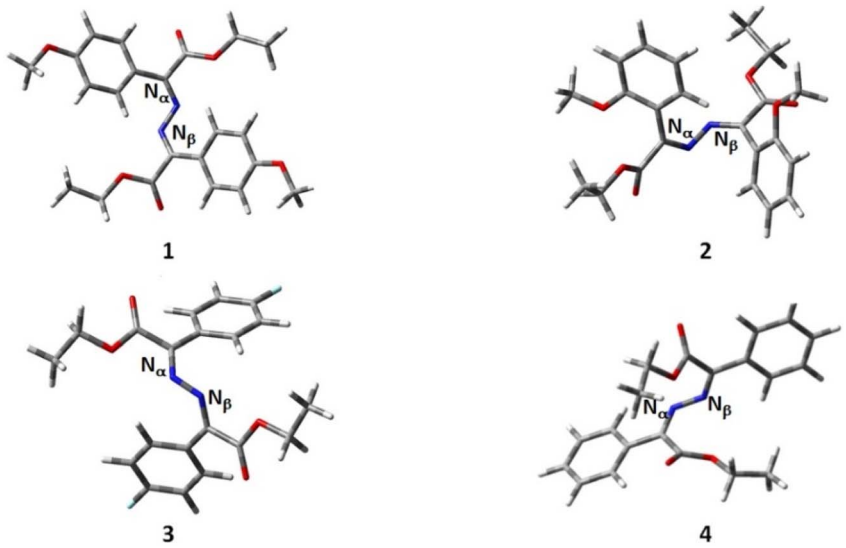

Fig. 7 Optimized geometries of the diazines **1–4**.

Table 4 Effect of the solvents on the absorption spectra of the synthesized compounds (DFT study)

	λ_{abs} (nm)			
Solvent systems	**1**	**2**	**3**	**4**
Gas phase	402, 299	385, 305	314	312
CH_3OH	402, 298	383, 304	314	312
CH_3CN	403, 298	384, 305	313	312
DMSO	404, 299	384, 304	314	313
DCM	402, 298	380, 302	314	313
THF	402, 301	379, 302	314	313
Hexane	398, 301	367, 295	313	312

Table 5 Absorption energies (eV) of the synthesized compounds in different solvents

	Absorption energies (eV)							
	1		**2**		**3**		**4**	
Solvent systems	Expt.	Theory	Expt.	Theory	Expt.	Theory	Expt.	Theory
CH_3OH	3.96	4.76	4.33	5.05	4.60	4.81	4.37	4.83
CH_3CN	4.05	4.76	4.18	5.05	4.41	4.80	3.89	4.83
DMSO	3.99	4.76	4.44	5.05	3.81	4.81	3.88	4.83
DCM	3.92	4.76	4.57	5.06	3.85	4.83	3.91	4.83
THF	4.07	4.76	4.20	5.06	3.79	4.86	4.09	4.83
Hexane	4.01	4.77	4.49	5.06	3.85	4.98	4.02	4.84

The FMO analysis shows that for **1**, HOMO−1 is located over the phenyl ring–nitrogen atom of the diazine unit and the oxygen atom of the methoxy group, and LUMO+1 is spread over the carbonyl carbon-imine carbon and the nitrogen atoms of the diazine in all solvents. For **2**, in the case of all solvent systems, except in hexane, HOMO−1 spreads over the phenyl ring-nitrogen atom and the oxygen atom of the methoxy group with a minimum electron density over the nitrogen atoms, and LUMO+1 is spread over the carbonyl carbon-imine carbon and the nitrogen atom of the diazine. However, in the case of hexane, HOMO−1 is located over the only phenyl ring and the oxygen atom of the substituted methoxy group of the symmetrical diazine. For **3**, in all the solvents, HOMO−1 is spread over the phenyl ring and the fluorine and nitrogen atoms of the diazine, and LUMO+1 is spread over the carbonyl carbon-imine carbon and the nitrogen atom of the diazine. In the case of **4**, HOMO−1 is spread over the phenyl ring and the nitrogen atom of the diazine moiety, and LUMO+1 is spread over the carbonyl carbon-imine carbon and the nitrogen atom of the diazine in all solvents (Fig. S6 and Table S1). The energy of the absorption spectra of the corresponding transition is calculated for both the experimental and theoretical methods. Both the calculated and experimental values were in good agreement (Tables 4 and 5).

Table 6 Calculated absorption maxima (nm) of the compounds **1–4** in the gas phase and hexane using the B3LYP and CAM-B3LYP theories

	λ_{abs} (nm)			
	Gas phase		Hexane	
Solvent systems	B3LYP	CAM-B3LYP	B3LYP	CAM-B3LYP
1	402, 299	400, 296	398, 301	402, 298
2	385, 305	378, 299	367, 295	371, 300
3	314	312	313	311
4	312	308	312	306

The energy of the absorption spectra using the B3LYP and CAM-B3LYP theories was calculated for **1–4** in the gas phase and hexane as a solvent. The absorption values were comparable for both theories (Table 6). NBO analysis shows that both C_α and C_β is doubly bonded with N_α and N_β, respectively with maximum contribution from nitrogen atom; and in all cases p orbital contributes more than s and d-orbitals (Table S1).

Table 7 FMO analysis

Solvent system	HOMO-1 (Hartree)	LUMO+1 (Hartree)	Energy (eV)	Solvent system	HOMO−1 (Hartree)	LUMO+1 (Hartree)	Energy (eV)
1-CH_3OH	−0.245	−0.069	4.789	**3**-CH_3OH	−0.238	−0.062	4.789
1-CH_3CN	−0.245	−0.070	4.762	**3**-CH_3CN	−0.238	−0.062	4.789
1-DMSO	−0.245	−0.070	4.762	**3**-DMSO	−0.239	−0.062	4.816
1-DCM	−0.245	−0.068	4.816	**3**-DCM	−0.237	−0.059	4.844
1-THF	−0.243	−0.068	4.762	**3**-THF	−0.237	−0.058	4.871
1-Hexane	−0.240	−0.064	4.789	**3**-Hexane	−0.233	−0.050	4.980
2-CH_3OH	−0.237	−0.051	5.061	**4**-CH_3OH	−0.251	−0.073	4.844
2-CH_3CN	−0.237	−0.052	5.034	**4**-CH_3CN	−0.251	−0.073	4.844
2-DMSO	−0.238	−0.051	5.088	**4**-DMSO	−0.251	−0.073	4.844
2-DCM	−0.236	−0.050	5.061	**4**-DCM	−0.250	−0.073	4.816
2-THF	−0.235	−0.049	5.061	**4**-THF	−0.250	−0.072	4.844
2-Hexane	−0.231	−0.044	5.088	**4**-Hexane	−0.248	−0.071	4.816

Conclusions

The photophysical study of **1–4** is reported herein. The study shows that the polarity of the solvents does not have a relatively great influence on λ_{abs}; however, λ_{em} increases with the polarity of the solvent. The addition of metal ions induced a blue shift of λ_{max} with a simultaneous increase in the absorption intensity; Pb showed the maximum absorption intensity. Hence, the synthesized diazine could be a potential molecule for detecting Pb^{2+} ions. However, the emission intensity decreased after the addition of the metal ions. The experiment was further supported by computational studies, and the experimental data were in good agreement with the theoretical data. TDDFT study shows that for all the compounds, the λ_{abs} corresponds to the HOMO−1 to LUMO+1 transition.

Experimental section

General information

Compounds **1–4** were synthesized as per the reported general procedure. The AR-grade solvents used for the UV-vis and photoluminescence studies were procured from Sisco Research Laboratory, India, and used as received without any further purification. $CuCl_2$, $PbCl_2$, $NiCl_2$ and $CoCl_2$ were procured from Avra Synthesis, India. A stock solution of 1 M was prepared for the compounds **1–4** in different solvents and was further diluted to 1 μM for the UV-vis and photoluminescence studies. The influence of the metal ions on the UV-vis and emission spectra was studied by adding a 1 mM DCM solution of the metal ions (Pb^{2+}, Cu^{2+}, Co^{2+} and Ni^{2+}) to compound **4** (0.5 mL:9.5 mL). The UV-visible spectra were recorded using standard 1 cm quartz cells on a Shimadzu UV-2450 spectrophotometer. The photoluminescence spectra were recorded using standard 1 cm quartz cells on a Jobin Yvon FLUOROLOG-FL3-11 spectrofluorometer; the compounds were excited at their absorption maxima to record the emission spectra.

Author contributions

All the authors contributed equally.

Conflicts of interest

There are no conflicts to declare.

Data availability

The data that support the findings of this study are available in the supplementary information (SI) of this article. Supplementary information is available. See DOI: https://doi.org/10.1039/d6ra00637j.

Acknowledgements

C. S. gratefully acknowledges the Anusandhan National Research Foundation (ANRF), New Delhi, India, for the financial support (ANRF/PAIR/2025/000021/PAIR). We thank the Central Instrumentation Facility, Pondicherry University, for the UV-vis and fluorescence spectroscopy instruments.

Notes and references

1 (*a*) S. Achelle and C. Baudequin, *Targets Heterocycl. Syst.*, 2013, **17**, 1; (*b*) S. Achelle, C. Baudequin and N. Plé, *Dyes Pigm.*, 2013, **98**, 575–600; (*c*) S. Achelle, J.-L. Rodríguez, C. Katan and F. R. le Guen, *J. Phys. Chem. C*, 2016, **120**, 26986; (*d*) M. Hodée, A. Lenne, J.-L. Rodriguez, F. R. Guen, C. Katan, S. Achelle and A. Fihe, *New J. Chem.*, 2021, **45**, 19132.

2 (*a*) X. J. Xu, S. Y. Chen, G. Yu, C. A. Di, H. You, D. G. Ma and Y. Q. Liu, *Adv. Mater.*, 2007, **19**, 1281; (*b*) Z. Q. Gao, B. X. Mi, H. L. Tam, K. W. Cheah, C. H. Chen, M. S. Wong, S. T. Lee and C. S. Lee, *Adv. Mater.*, 2008, **20**, 774; (*c*) M. Ghasemi, J. Cameron, W. K. Lin, D. Volyniuk, P. J. Skabara, J. V. Grazulevicius and G. Sini, *Adv. Opt. Mater.*, 2025, **13**, e01829.

3 (*a*) S. Furumi and K. Ichimura, *J. Phys. Chem. B*, 2007, **111**, 1277–1287; (*b*) G. W. Gray and S. M. Kelly, *J. Mater. Chem.*, 1999, **9**, 2037; (*c*) J. Chen, T. Xu, W. Zhao, L.-L. Ma, D. Chen and Y.-Q. Lu, *Polymer*, 2021, **218**, 123492; (*d*) X. Xi, C. Yan, L. Z. Shen, Y. Wang and P. Cheng, *Mater. Today Electron.*, 2023, **6**, 100069.

4 (*a*) R. Glaser, G. S. Chen, M. Anthamatten and C. L. Barnes, *J. Chem. Soc., Perkin Trans. 2*, 1995, **7**, 1449; (*b*) K. J. Wallace, J. Morey, V. M. Lyncha and E. V. Anslyn, *New J. Chem.*, 2005, **29**, 1469–1474; (*c*) M. Revanasiddappa, T. Suresh, S. Khasim, S. C. Raghavendra, C. Basavaraja and S. D. Angadi, *J. Chem.*, 2008, **2**, 395; (*d*) S. S. Chourasiya, D. Kathuria, A. A. Wania and P. V. Bharatam, *Org. Biomol. Chem.*, 2019, **17**, 8486–8521.

5 (*a*) J. Safari, S.-R. Gandomi, J. Hai-Zhen, R. Zhong-jiao, W. Wen and S. Long-gang, *J. Shanghai Univ.*, 2005, **4**, 369; (*b*) H. Zachová, S. Man, J. Taraba and M. Potáček, *Tetrahedron*, 2009, **65**, 792; (*c*) L. R. de Almeida, P. S. Carvalho, H. B. Napolitano, S. S. Oliveira, A. J. Camargo, A. S. Figueredo, G. L. B. de Aquino and V. H.-S. Carvalho, *Cryst. Growth Des.*, 2017, **17**, 5145.

6 (*a*) A. R. Kennedy, K. G. Brown, D. Graham, J. B. Kirkhouse, M. Kittner and C. Major, *New J. Chem.*, 2005, **29**, 826; (*b*) D. Dragancea, V. B. Arion, S. Shova, E. Rentschler and N. V. Gerbeleu, *Angew. Chem., Int. Ed. Engl.*, 2005, **44**, 7938; (*c*) D. Sek, M. Siwy, K. Bijak, M.-Z. Grucela, G. Malecki, K. Smolarek, L. Bujak, S. Mackowski and E.-B. Schab, *J. Phys. Chem. A*, 2013, **117**, 10320; (*d*) V. Ch. Kravtsov, V. Lozovan, N. Siminel, E. B. Coropceanu, O. V. Kulikova, N. V. Costriucova and M. S. Fonari, *Molecules*, 2020, **25**, 5616.

7 (*a*) R. Centore, B. Panunzi, A. Roviello, A. Sirigu and P. Villano, *Mol. Cryst. Liq. Cryst.*, 1996, **275**, 107; (*b*) E. C. Kesslen, *Tetrahedron Lett.*, 1995, **36**, 4725; (*c*) W. B. Euler, in *Handbook of Organic Conductive Molecules and Polymers; Synthesis and Electrical Properties*, Wiley, New York, 1997, vol. 719; (*d*) A. G. Osborne, S. M. Webba Da, M. B. Hursthouse, K. M. A. Malik, G. Opromolla and P. Zanello, *J. Organomet. Chem.*, 1996, **516**, 167; (*e*) M. ustafa Emirik, K. Karaoğlu, K. Serbest, U. Çoruh and E. M. V. Lopez, *Polyhedron*, 2015, **88**, 182; (*f*) E. Rahali, Z. Noori, Y. Arfaoui and J. Poater, *Int. J. Mol. Sci.*, 2024, **25**, 7497.

8 (*a*) J. Ardaraviciene, B. Barvainiene, T. Malinauskas, V. Jankauskas, K. Arlauskas and V. Getautis, *React. Funct. Polym.*, 2011, **71**, 1016; (*b*) P. A. Sobarzo, I. A. Jessop, Y. Pérez, R. A. Hauyon, M. V.-T. Velázquez, J. Medina, A. González, L. E. García, C. M.-H. González, D. Coll, P. A. Ortiz, A.-C. Tundidor and C. A. Terraza, *J. Appl. Polym. Sci.*, 2022, **139**, e52911.

9 (*a*) N. Narayanaswamy and T. Govindaraju, *Sens. Actuators, B*, 2012, **161**, 304; (*b*) Z. Gong, R. Wang, Y. Jiang, X. Kong, Y. Lin and Z. Xu, *Org. Electron.*, 2021, **92**, 106102.

10 (*a*) S. Yan, R. Huang, Y. Zhou, M. Zhang, M. Deng, X. Wang, X. Weng and X. Zhou, *Chem. Commun.*, 2011, **47**, 1273; (*b*) A. Boländer, D. Kiesner, C. Voss, S. Bauer, C. Schön, S. Burgold, T. Bittner, J. Hölzer, R. H. Heyny-von, G. Mall, V. Goetchy, C. Czech, H. Knust, R. Berber, J. Herms, I. Hilger and B. Schmidt, *J. Med. Chem.*, 2012, **55**, 9170; (*c*) A. Lyčka, G. Noirbent and S. Achelle, *J. Mol. Struct.*, 2026, **1350**, 143980.

11 (*a*) M. U. Anwar, L. K. Thompson, L. N. Dawe, F. Habib and M. Murugesu, *Chem. Commun.*, 2012, **48**, 4576; (*b*) L. K. Thompson, *Coord. Chem. Rev.*, 2002, **233–234**, 193; (*c*) X. Wang, Y. Yong, W. Yang, A. Zhang, X. Xie, P. Zhu and Y. Kuang, *ACS Omega*, 2021, **6**, 11418.

12 (*a*) C. Hadad, S. Achelle, S. I. Lopez, M. J. Garcia and L. J. Rodriguez, *Dyes Pigm.*, 2013, **97**, 230; (*b*) M. Hruzd, R. Durand, S. Gauthier, P. le Poul, F. R. le Guen and S. Achelle, *Chem. Rec.*, 2024, **24**, e202300335; (*c*) W. Ali, H. Bakhshi, A. Jabbar, M. Pilkington, J. M. Rawson, A. Al-Harrasi and M. U. Anwar, *Dalton Trans.*, 2026, **55**, 114.

13 (*a*) M. U. Anwar, A. Al-Harrasi, E. L. Gavey, M. Pilkington, J. M. Rawson and L. K. Thompson, *Dalton Trans.*, 2018, **47**, 2511; (*b*) S. Achelle, L. J. Rodriguez, F. Bureš and F. RobinleGuen, *Chem. Rec.*, 2020, **20**, 440.

14 (*a*) F. Chevallier and F. Mongin, *Chem. Soc. Rev.*, 2008, **37**, 595–609; (*b*) J. Singh, S. K. Panda and A. K. Singh, *RSC Adv.*, 2022, **12**, 18945.

15 (*a*) Z. Xu, L. K. Thompson and D. O. Miller, *Inorg. Chem.*, 1997, **36**, 3985–3995; (*b*) L. K. Thompson, Z. Xu, A. E. Goeta, J. A. K. Howard, H. J. Clase and D. O. Miller, *Inorg. Chem.*, 1998, **37**, 3217–3229; (*c*) V. A. Milway, V. Niel, T. S. M. Abedin, Z. Xu, L. K. Thompson, H. Grove, D. O. Miller and S. R. Parsons, *Inorg. Chem.*, 2004, **43**, 1874–1884; (*d*) R. E. P. Winpenny, *Chem. Soc. Rev.*, 1998, **27**, 447.

16 (*a*) G. Ge, J. He, H. Guo, F. Wang and D. Zou, *J. Organomet. Chem.*, 2009, **694**, 3050–3057; (*b*) M. Panigati, M. Mauro, D. Donghi, P. Mercandelli, P. Mussini, L. De Cola and G. D'Alfonso, *Coord. Chem. Rev.*, 2012, **256**, 1621–1643; (*c*) M. U. Anwar, A. Al-Harrasi, M. Pilkington, E. L. Gavey and J. M. Rawson, *Polyhedron*, 2019, **165**, 63–67; (*d*) M. U. Anwar, A. Al-Harrasi, E. L. Gavey, M. Pilkington, J. M. Rawson and L. K. Thompsond, *Dalton Trans.*, 2018, **47**, 2511.

17 (*a*) L. K. Thompson and L. N. Dawe, *Coord. Chem. Rev.*, 2015, **289–290**, 13–31; (*b*) M. Yahiaoui, S. Tabti, A. Guerraoui, A. Djedouani, D. Hannachi, M. Laidoudi, I. Warad, H. – E. Stoeckli, S. Fleutot, T. M. Almutairi and M. S. Islam, *Mol. Phys.*, 2025, **123**, e2446686.

18 (*a*) Z. Xu, L. K. Thompson and D. O. Miller, *Inorg. Chem.*, 1997, **36**, 3985; (*b*) S. Gupta and S. S. Pal, *Inorg. Chem.*, 2005, **44**, 6299; (*c*) S. Shi, T. M. Yao, X. T. Geng, L. Chen and L. N. Ji, *Acta Crystallogr., Sect. E: Struct. Rep. Online*, 2007, **64**, o272; (*d*) W. Huang, Y. Jin, D. Wu and G. Wu, *Inorg. Chem.*, 2014, **53**, 73.

19 (*a*) M. U. Anwar, J. M. Rawson, E. L. Gavey, M. Pilkington, A. Al-Harrasia and L. K. Thompsond, *Dalton Trans.*, 2017, **46**, 2105; (*b*) M. U. Anwar, A. Al-Harrasi, M. Pilkington, E. L. Gavey and J. M. Rawson, *Polyhedron*, 2019, **165**, 63–67; (*c*) H. Grove, T. L. Kelly, L. K. Thompson, L. Zhao, Z. Xu, T. S. M. Abedin, D. O. Miller, A. E. Goeta, C. Wilson and J. A. K. Howard, *Inorg. Chem.*, 2004, **43**(14), 4278; (*d*) L. K. Thompson, Z. Xu, A. E. Goeta, J. A. K. Howard, H. J. Clase and D. O. Miller, *Inorg. Chem.*, 1998, **37**, 3217.

20 (*a*) N. S. Hush and J. R. Reimers, *Chem. Rev.*, 2000, **100**, 775; (*b*) E. A. Okba, Y. M. Hanafi, T. A. Fayed, A. S. Mahmoud Sakr and A. Samy El-Daly, *Sci. Rep.*, 2025, **15**, 33329.

21 M. C. Bagley, Z. Lin and S. J. A. Pope, *Tetrahedron Lett.*, 2009, **50**, 6818.

22 (*a*) F. Lincker, D. Kreher, A.-J. Attias, J. Do, E. Kim, P. Hapiot, N. Lemaître, B. Geffroy, G. Ulrich and R. Ziessel, *Inorg. Chem.*, 2010, **49**, 3991; (*b*) R. F. Landis, M. Yazdani, B. Creran, X. Yu, V. Nandwana, G. Cookeb and V. M. Rotello, *Chem. Commun.*, 2014, **50**, 4579.
23 V. Schmitt, S. Moschel and H. Detert, *Eur. J. Org Chem.*, 2013, **2013**, 5655.
24 C. Wink and H. Detert, *J. Phys. Org. Chem.*, 2013, **26**, 144–150.
25 P. Singh, A. Baheti and K. R. J. Thomas, *J. Org. Chem.*, 2011, **76**, 6134–6145.
26 S. Achelle, A. Barsella, C. Baudequin, B. Caro and R. F. le Guen, *J. Org. Chem.*, 2012, **77**, 4087–4096.
27 S. Achelle, I. Nouira, B. Pfaffinger, Y. Ramondenc, N. Ple and L. J. Rodríguez, *J. Org. Chem.*, 2009, **74**, 3711–3717.
28 S. Achelle, L. J. Rodríguez and G. F. Robin-le, *J. Org. Chem.*, 2014, **79**, 7564–7571.
29 S. Achelle, L. J. Rodríguez, F. Bures and G. F. Robin-le, *Dyes Pigm.*, 2015, **121**, 305–311.
30 (*a*) C. Hadad, S. Achelle, S. I. Lopez, M. J. C. García and L. J. Rodríguez, *Dyes Pigm.*, 2013, **97**, 230; (*b*) S. Achelle, J. Rodríguez-Lopez, C. Katan and F. Robin-le Guen, *J. Phys. Chem. C*, 2016, **120**, 26986.
31 (*a*) M. Guo, M. Li, Y. Dai, W. Shen, J. Peng, C. Zhu, S. H. Lin and R. He, *RSC Adv.*, 2013, **3**, 17515–17526; (*b*) M.-Y. Guo, R.-X. He, Y.-L. Dai, W. Shen, M. Li, C.-Y. Zhu and S.-H. Lin, *J. Phys. Chem. C*, 2012, **116**, 9166–9179; (*c*) S.-H. Chou, C.-H. Tsai, C.-C. Wu, D. Kumar and K.-T. Wong, *Chem.–Eur. J.*, 2014, **20**, 16574–16582; (*d*) L.-Y. Lin, C.-H. Tsai, K.-T. Wong, T.-W. Huang, C.-C. Wu, S.-H. Chou, F. Lin, S.-H. Chen and A. –I. Tsai, *J. Mater. Chem.*, 2011, **21**, 5950–5958.
32 M. Hruzd, R. Durand, S. Gauthier, P. le Poul, F. Robin-le Guen and S. Achelle, *Chem. Rec.*, 2024, **24**, e202300335.
33 (*a*) J. L. Gohres, C. L. Shukla, A. V. Popov, R. Hernandez, C. L. Liotta and C. A. Eckert, *J. Phys. Chem. B*, 2008, **112**, 14993; (*b*) B. Mennucci, *J. Am. Chem. Soc.*, 2002, **124**, 1506.
34 (*a*) S.-W. Chiu, L.-Y. Lin, H.-W. Lin, Y.-H. Chen, Z.-Y. Huang, Y.-T. Lin, F. Lin, Y.-H. Liu and K.-T. Wong, *Chem. Commun.*, 2012, **48**, 1857–1859; (*b*) C. C. Pérez, M. M. Oliva, J. T. L. Navarrete, J. P. Sestelo, M. M. Martínez and L. A. Sarandeses, *J. Org. Chem.*, 2019, **84**, 8870; (*c*) J. Issac, S. Ravi, K. Chidambaranathan, S. Karthikeyan, M. Pannipara, A. G. Al-Sehemi, S. P. Anthony and V. Madhu, *Cryst. Growth Des.*, 2024, **24**, 3388.
35 P. K. Madarasi and C. Sivasankar, *Appl. Organomet. Chem.*, 2022, **36**, e6522.
36 (*a*) E. V. Verbitskiy, A. V. Schepochkin, N. I. Makarova, I. V. Dorogan, A. V. Mitelitsa, V. I. Minkin, S. A. Kozyukhin, V. V. Emets, V. A. Grindgerg, O. N. Chupakhin, G. L. Rusinov and V. N. Charushin, *J. Fluoresc.*, 2015, **25**, 763–775; (*b*) L. Skarziute, J. Dodonova, A. Voichovicius, J. Jovaisaite, R. Komskis, A. Voitechoviciute, J. Bucevicius, K. Kazlaukas, S. Jursenas and S. Tumkevicius, *Dyes Pigm.*, 2015, **118**, 118–128; (*c*) S. Kato, Y. Yamada, H. Hiyoshi, K. Umezu and Y. Nakamura, *J. Org. Chem.*, 2015, **80**, 9076–9090; (*d*) K. Hoffert, R. J. Durand, S. Gauthier, F. Robin -le Guen and S. Achelle, *Eur. J. Org Chem.*, 2017, **2017**, 523–529; (*e*) J. Achelle, L. Rodríguez and G. F. Robin-le, *J. Org. Chem.*, 2014, **79**, 7564–7571; (*f*) S. Achelle, A. Barsella, C. Baudequin, B. Caro and F. Robin-le Guen, *J. Org. Chem.*, 2012, **77**, 4087–4096; (*g*) V. Schmitt, S. Moschel and H. Detert, *Eur. J. Org Chem.*, 2013, **2013**, 5655–5669.
37 C. Reichardt, *Chem. Rev.*, 1994, **94**, 2319–2358.
38 (*a*) A. A. Saddik, A. A. K. Mohammed, S. K. Talloj, A. M. K. El-Deana and O. Younis, *RSC Adv.*, 2024, **14**, 6072; (*b*) S. Prabu and N. Palanisami, *Dyes Pigm.*, 2022, **201**, 110193; (*c*) T. Coradin, R. Clément, P. G. Lacroix and K. Nakatani, *Chem. Mater.*, 1996, **8**, 2153.
39 (*a*) E. V. Verbitskiy, Y. A. Kvashnin, A. A. Baranova, K. O. Khokhlov, R. D. Chuvashov, I. E. Schapov, Y. A. Yakovleva, E. F. Zhilina, A. V. Shchepochkin, N. I. Makarova, E. V. Vetrova, A. V. Metelitsa, G. L. Rusinov, O. N. Chupakhin and V. N. Charushin, *Dyes Pigm.*, 2020, **178**, 108344; (*b*) J. Magyari, B. B. Holló, M. V. Rodić, L. S. Jovanović, K. M. Szécsényi, W. Ferenc, D. Osypiuk, T. Mosolygó, A. Kincses and G. Spengler, *J. Therm. Anal. Calorim.*, 2022, **147**, 229.
40 (*a*) R. Lartia, C. Allain, B. Bordeau, F. Schmidt, D. C. Fiorini, F. Charra and F. M.-P. Teulade, *J. Org. Chem.*, 2008, **73**, 1732; (*b*) C. Le Droumaguet, A. Sourdon, E. Genin, O. Mongin and D. M. Blanchard, *Chem.–Asian J.*, 2013, **8**, 2984–3001; (*c*) A. Tigreros, A. Ortiz and B. Insuasty, *Dyes Pigm.*, 2014, **111**, 45–51; (*d*) E. Ishow, R. Guillot, G. Buntinx and O. Poizat, *J. Photochem. Photobiol., A*, 2012, **234**, 27–36; (*e*) E. Ishow, G. Clavier, F. Miomandre, M. Rebarz, G. Buntinx and O. Poizat, *Phys. Chem. Chem. Phys.*, 2013, **15**, 13922–13939; (*f*) R. Ghosh and B. Mannaa, *Phys. Chem. Chem. Phys.*, 2017, **19**, 23078; (*g*) J. Jia, J. Li, T. Zhang, Y. Lub and Y. Song, *Phys. Chem. Chem. Phys.*, 2024, **26**, 11064.
41 A. D. J. Becke, *Chem. Phys.*, 1993, **98**, 5648–5652.
42 A. D. J. Becke, *Chem. Phys.*, 1993, **98**, 1372–1377.
43 A. D. Becke, *Phys. Rev. A*, 1988, **38**, 3098–3100.
44 P. C. Hariharan and J. A. Pople, *Mol. Phys.*, 1974, **27**, 209–214.
45 P. C. Hariharan and J. A. Pople, *Theor. Chim. Acta*, 1973, **28**, 213–222.
46 W. J. Hehre, R. Ditchfield and J. A. Pople, *J. Chem. Phys.*, 1972, **56**, 2257–2261.
47 R. Ditchfield, W. J. Hehre, J. A. Pople, W. J. Hehre, K. Ditchfield and J. A. Pople, *J. Chem. Phys.*, 1971, **54**, 724–728.
48 B. Mennucci and J. Tomasi, *J. Chem. Phys.*, 1996, **106**, 5151–5158.
49 D. M. Chipman, *J. Chem. Phys.*, 2000, **112**, 5558–5565.
50 A. V. Marenich, J. C. Cramer and G. D. Truhlar, *J. Phys. Chem. B*, 2009, **113**, 6378–6396.
51 J. Tomasi, B. Mennucci and R. Cammi, *Chem. Rev.*, 2005, **105**, 2999–3094.
52 D. M. Chipman, *Theor. Chem. Acc.*, 2002, **107**, 80–89.
53 R. D. Dennington, T. A. Keith and J. M. Millam, *GaussView 5.0. 8*, Gaussian Inc., Wallingford, 2008.
54 (*a*) T. Yanai, D. P. Tew and N. C. Handy, *Chem. Phys. Lett.*, 2004, **393**, 51; (*b*) D. Hall, J. C. Sancho-García, A. Pershin, D. Beljonne, E.-C. Zysman and Y. Olivier, *J. Phys. Chem. A*, 2023, **127**, 4743.